

A NEW MAGNETICALLY ACTUATED MICROVALVE FOR LIQUID AND GAS CONTROL APPLICATIONS

Daniel J. Sadler, Kwang W. Oh, Chong H. Ahn, Shekhar Bhansali, and H. Thurman Henderson
Center for Microelectronic Sensors and MEMS
Department of Electrical and Computer Engineering and Computer Science
University of Cincinnati
P.O. Box 210030, Cincinnati, OH 45221-0030 U.S.A
Phone: (513) 556-1997, Fax: (513) 556-7326.
Email: dsadler@ececs.uc.edu

ABSTRACT

In this paper, we describe the design, fabrication, and testing of a prototype microvalve which makes use of a novel magnetic microactuator. The completed device consists of three layers, with the bottom two layers making up the normally closed valve. The top layer (actuator) contains the flux generator on its top surface combined with Ni/Fe plated through holes for guiding the flux to the valve. The actuator and valve components are separately fabricated and then mounted onto a glass motherboard which contains both fluid flow channels and patterned gold traces for making electrical connections. In addition to providing an easy means for testing, the motherboard will allow for the later attachment of other microfluidic components to create a complete microfluidic total analysis system (μ TAS) on a single substrate. Preliminary test results show that the valve is capable of controlling gas and liquid flow in the range of submicroliters to hundreds of μ L/min.

INTRODUCTION

There has been a growing interest in microfluidic components such as valves and pumps for use in various microfluidic systems. In this work, we have designed, fabricated, and tested a new magnetically driven prototype microvalve. Many types of valves and have been reported using various actuation schemes [1-7], including a magnetically actuated valve, which our group recently reported at the SPIE microfluidics conference [7]. This new valve retains the many advantages described in our previous paper and also includes some significant improvements. Valve seats have been added to decrease both the steady-state leak rate and the amount of current required to actuate the valve. A glass motherboard has also been developed which contains flow channels as well as gold traces for making electrical contacts. In addition to improving testing and assembly, this motherboard will allow for easy interfacing of the newly developed valves with other

microfluidic components such as pumps, sensors, and bio-filters, thereby enabling the development of a complete microfluidic total analysis system (μ TAS) on a single substrate. Finally, these two improvements have enabled us to better characterize the new valves, allowing us to present preliminary data for the performance in gas as well as liquid control applications.

DESIGN

A cut-view schematic representation of the device mounted on a glass motherboard is shown in Figure 1. For the valve layers, inlets, outlets, and valve seats are patterned on a glass wafer that is electrostatically bonded to a silicon wafer. The inlet and outlet, which are 3000 μ m apart, are each circular with a radius of 340 μ m. Both have a valve seat which is raised by about 3 μ m. The silicon wafer contains an anisotropically etched, 10 μ m-thick silicon membrane which is 3000 μ m x 5000 μ m. The top of the membrane is coated with a 2000 μ m x 2000 μ m x 7 μ m square of electroplated Ni/Fe permalloy.

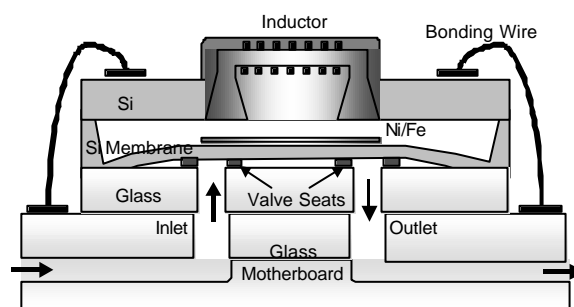


Figure 1. Normally closed magnetic microvalve shown with both fluidic and electrical connections made to a glass motherboard.

The top layer of the device contains the actuator, which consists of the flux generator on its top surface combined with Ni/Fe plated through holes for guiding the flux to the valve. The flux generator is a

horseshoe-shaped inductor with a 25 μm -thick magnetic core that has a width of 600 μm and a total length of 8000 μm . It accommodates 60 turns of copper coils and has four through-holes which are 400 μm x 400 μm each. By guiding magnetic flux through the wafer, the through-holes, or magnetic vias, allow precise control and reduction of the air gap in the driving magnetic circuit. This air gap reduction leads to a decrease in power required to drive the magnetic actuator. Also, because the flux generator is fabricated on the side opposite where actuation occurs, the actuator can be readily connected to driving circuitry without interfering with the actuating device. This is especially important in microfluidic applications which have liquids flowing through valves and channels.

The actuator, valve components, and the glass motherboard are separately fabricated and the complete device is then realized by attaching the separate components using special low temperature bonding methods.

FABRICATION

Brief fabrication steps for the actuator, and for the valve and motherboard are shown in Figures 2 and 3 respectively. For complete fabrication steps of the magnetic actuator, please see [7] and [8], as the fabrication steps will only be briefly mentioned in this section. For the actuator, the process consisted of first etching and electroplating magnetic vias or through-holes, and then building the inductor on top of the through-hole wafer using a multi-layer thick photoresist process. Through-holes are patterned onto the backside of an n-type, (100) oriented, 250 μm -thick silicon wafer using standard photolithography and are then etched in a 45% KOH solution. After etching is completed, the empty through-holes are electroplated with Ni/Fe (81%/19%) permalloy using a backside Cr/Cu/Cr metal layer as an electroplating seed layer. The through-holes are plated until they reach the top of the wafer, thus forming the magnetic vias, which allow magnetic flux to pass through the silicon wafer. After the magnetic vias are complete, the inductor is ready to be fabricated on the topside of the wafer.

Inductor fabrication on top of the through-hole wafer is based on a thick photoresist process recently developed at the University of Cincinnati [8]. AZ-4000 series photoresist is used to produce a 25 μm thick electroplating mold. Copper lines are then electroplated to the top of the mold from an underlying Ti/Cu seed using standard electroplating techniques. After removing the photoresist and seed layer, a new layer of photoresist is spun, via openings

are patterned, and the photoresist is hard cured at 220 $^{\circ}\text{C}$ to form a permanent and planarizing dielectric layer. Another seed layer is then deposited from which first vias and then a magnetic core are patterned and electroplated. Conductor vias are electroplated copper with a cross section of 50 μm x 50 μm and a thickness of 25 μm . The magnetic core is formed from electroplated Ni/Fe (81%/19%) permalloy and is also 25 μm thick. Then photoresist and seed layers are removed, and another hard curing is performed. Finally, top conductor lines are patterned and grown from another seed layer in exactly the same method as the bottom conductors. Again, conductor thickness is 25 μm .

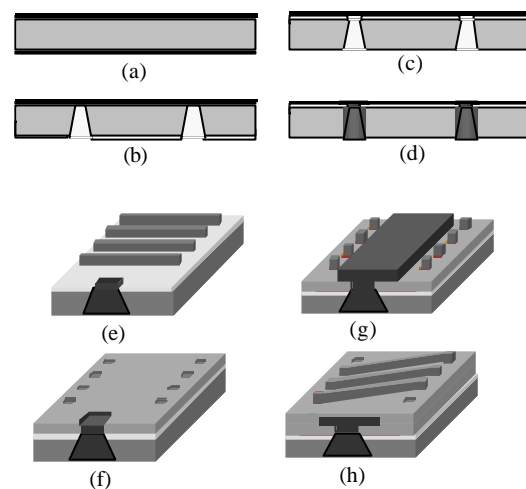


Figure 2. Magnetic actuator fabrication steps: (a) Silicon wafer with Cr/Cu seed layer; (b) Through-hole etch in KOH; (c) Oxide removal; (d) Ni/Fe through-hole plating; (e) Electroplating of thick copper conductor lines; (f) Via opening and photoresist hard-curing; (g) Electroplating of vias and magnetic core; and (h) Via opening on second photoresist layer, hard-curing, and top conductor line electroplating.

The fabrication of the valve components begins with a 2-inch (100) n-type silicon wafer which is only 50 μm -thick. Onto the wafer is grown about 5000 \AA of SiO_2 . The topside of the wafer is first patterned and etched in a 25% TMAH solution to a depth of 40 μm , thus defining a 10 μm -thick membrane. Meanwhile, 3 μm -thick valve seats are patterned onto a Pyrex glass wafer using PI-2721, a photosensitive polyimide. Next, 500 \AA of titanium is deposited and patterned using the liftoff method. Inlets and outlets are then drilled using 13-mil (330 micron) diameter diamond-tipped drills. This glass wafer is then electrostatically bonded to the previously mentioned membrane wafer. The exposed glass bonds easily to the silicon at a temperature of 400 $^{\circ}\text{C}$ and an applied potential of about 1.2 KV. Areas covered with

titanium, however, do not bond and therefore define the deflectable membrane. Finally, a seed layer is deposited, and a thin layer of Ni/Fe permalloy is electroplated onto the topside of the valve. This allows for a completed magnetic circuit between the electromagnetic actuator and the top of the valve, which produces the necessary force of attraction.

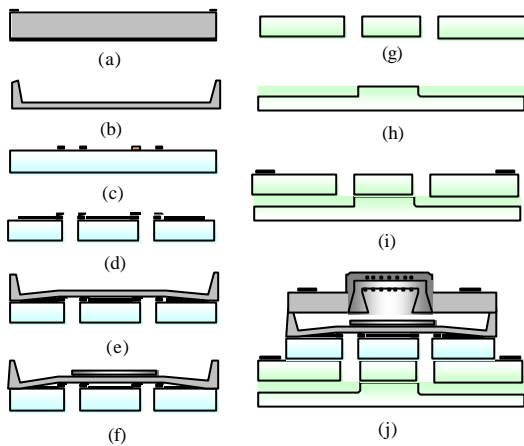


Figure 3. Valve fabrication steps: (a) Oxide Patterning on silicon wafer; (b) Membrane etching in TMAH; (c) Glass wafer with polyimide valve seats; (d) Ti deposition and drilling; (e) Electrostatic bonding; and (f) Ni/Fe permalloy electroplating. Motherboard fabrication steps: (g) Drilling; (h) Channel etching; and (i) Glass-glass bonding and patterning for electrical contacts. Assembly: (j) Bonding of valve to motherboard and actuator to valve.

Motherboard fabrication is accomplished by first patterning and etching two 250 μm -thick Pyrex glass wafers. An e-beam evaporated Cr/Au (400 \AA /4000 \AA) layer serves as an etch mask, and both wafers are etched in a concentrated HF solution. The top wafer is only briefly etched to reveal a template for the drilling of inlet and outlet holes. These holes are then drilled in the same manner as described for the valve. The bottom wafer, which defines the fluidic paths, is etched to form 100 μm -deep, 250 μm -wide channels that direct fluid flow around the motherboard. After removal of the metal layers, the two wafers are then bonded together using a high temperature (650 $^{\circ}\text{C}$) glass bonding technique. Finally, gold traces are patterned for electrical contacts. The traces are made from an e-beam evaporated Cr/Au (400 \AA /4000 \AA) layer and are patterned by the liftoff method.

After all components are fabricated, the valve wafer and electromagnetic actuator wafer are diced into individual components. The valve is then bonded to the glass motherboard using a special spin-on teflon material known as CYTOP. After spin-coating CYTOP onto the motherboard, the valve is carefully aligned. By simply curing the device at 170 $^{\circ}\text{C}$ for 5

minutes, a strong leak-tight bond is insured. Next, the actuator is attached using a low temperature wax bonding technique. Then, wires are bonded from the bonding pads of the actuator to the gold traces of the motherboard to allow for electrical connection to the device. Finally, plastic tubes, which serve as the inlet and outlet, are bonded to the motherboard with epoxy. The finished device, shown in Figure 4, is now ready for test.

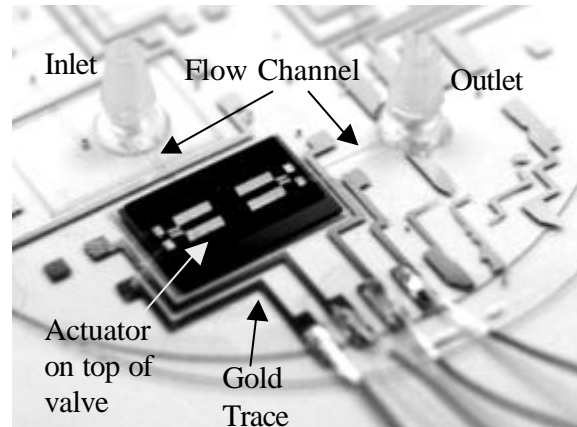


Figure 4. Photograph of assembled microvalve. Valve and actuator are attached to the glass motherboard which routes both electrical and fluidic connections.

RESULTS AND DISCUSSION

Upon completion of device fabrication, the performance of several devices was characterized using both nitrogen and DI water as the testing fluid. In the case of nitrogen, the gas was supplied by a pressurized nitrogen tank controlled with a precision regulator. For DI water, the supply pressure was varied by simply changing the water level in a supply reservoir. In both cases, a Motorola MPX2050 differential pressure sensor was used to measure the differential pressure across valve. For both nitrogen and DI water, we were able to measure the flow of fluid through the valve for various inlet pressures as a function of applied actuator current. Actuation current varied from 0 mA to 600 mA, and data was taken for various inlet pressures. Preliminary results are shown in Figures 5.

These preliminary results are quite promising, especially for the case of gas control. As is shown in the graphs, very low steady state leak rates of under 10 $\mu\text{L}/\text{min}$ have been achieved. The valves begin to turn on at an applied current of about 400 mA, and at 550 mA, the achievable flow rate is about 60 times the steady-state leak rate. For the case of DI water, the results are not quite as good, with leak rates around 0.2 $\mu\text{L}/\text{min}$ and an achievable flow of slightly

less than 1 $\mu\text{L}/\text{min}$. In both cases, performance seems to degrade at above 550 mA of applied actuator current possibly due to heating effects or saturation in the magnetic circuit. One major advantage of these devices is their low power consumption. Because of the low resistance of the inductors (about 1-ohm), the power consumption is only about 300 mW for an applied actuator current of 550 mA. The major problem we are experiencing is leakage. One factor that we believe contributes to this undesirable behavior is a stress mismatch between the silicon membrane and the electroplated Ni/Fe square. We are currently investigating this problem as well as other ways to prevent leakage in the closed mode.

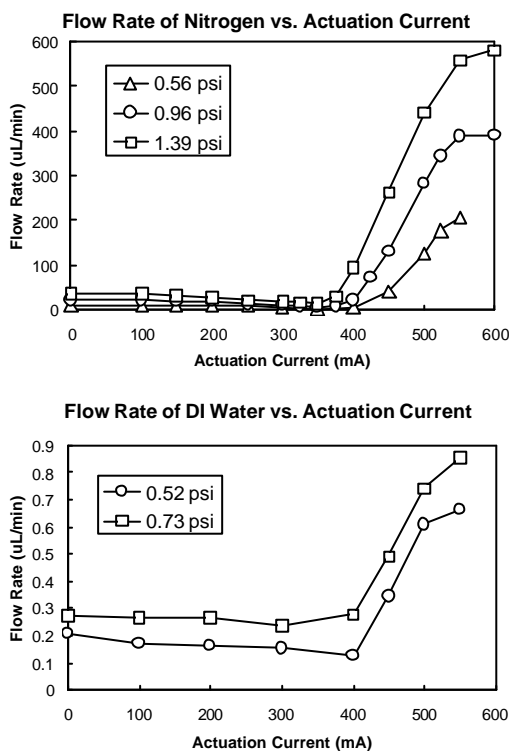


Figure 5. Measured flow Rate of Nitrogen and DI water vs. actuation current for different inlet pressures.

CONCLUSION

In this work, a prototype microvalve for both gas and liquid flow control using a new magnetic microactuator has been designed, fabricated, and tested. In addition, a glass motherboard containing both fluidic interconnects and electrical connections was also developed. Currently, there is much interest in the development of microfluidic components such as valves for microfluidic applications, and we believe that our device has many desirable features that will enable it to be useful in many such applications. The glass motherboard will allow for

the later attachment of other microfluidic components to create a complete microfluidic total analysis system (μTAS) on a single substrate. Initial characterization shows feasibility of the structure as a valve for controlling both gas and liquid flow in the range of microliters to hundreds of $\mu\text{L}/\text{min}$. Additional design changes are currently being investigated to prevent leakage in the closed mode. Since all of the components (actuator, valve, and motherboard) are fabricated separately, there is much flexibility for improvements and optimizations.

ACKNOWLEDGEMENT

This work was supported by the DARPA MicroFlumes Program (ETO) under contract number AF F30602-97-2-0102. The authors would also like to thank the Hoechst Celanese Company for their very generous donations of photoresist. Finally, we would like to thank Arum Han of the Center for Microelectronic Sensors and MEMS for his help with the glass motherboard fabrication.

REFERENCES

1. X. Q. Wang, Q. Lin, and Y.C. Tai, "A Parylene Micro Check Valve", *Proc. IEEE MEMS Workshop*, pp. 177-182, 1999.
2. C. A. Rich, and K.D. Wise, "An 8-Bit Microflow Controller Using Pneumatically-Actuated Microvalves", *Proc. IEEE MEMS Workshop*, pp. 130-134, 1999.
3. A. K. Henning et al., "Microfluidic MEMS for Semiconductor Processing", *IEEE Trans. On Components, Packaging, and Manufacturing Technology-Part B*, vol. 21, no. 4, pp.329-337, Nov. 1998.
4. K. D. Skrobaneck, M. Kohl, and S. Miyazaki, "Stress Optimised Shape Memory Microvalves", *Proc. IEEE MEMS Workshop*, pp. 256-261, 1997.
5. M. Stehr, S. Messner, H. Sandmaier, R. Zengerle, "The VAMP – a new device for handling liquids or gases", *Sensors and Actuators A* **57**, pp. 153-157, 1996.
6. D. Sim, T. Kurabayashi, and M. Esashi, "A bakable microvalve with a Kovar-glass-silicon-glass structure", *J. Micromech. Microeng.* **6**, pp. 266-271, 1996.
7. D. J. Sadler et al., "Prototype microvalve using a new magnetic microactuator", *Proc. SPIE Conference on Microfluidic Devices and Systems*, pp. 46-52, 1998.
8. M. Xu et al., "A microfabricated transformer for high-frequency power and signal conversion", *Proc. The 7th Joint MMM-Intermag Conference*, 1998.